Optical Properties of α-MnSe†*

Donald L. Decker‡ and R. L. Wild
University of California, Riverside, California 92502
(Received 23 November 1970)

Near-normal-incidence reflectance measurements are reported on the face-centered-cubic (fcc) phase of MnSe from 0.006 to 16 eV. The complex index of refraction and complex dielectric constant have been obtained from a Kramers-Kronig phase-shift dispersion analysis of normal-incidence reflectance data. The first-order infrared absorption (reststrahl) has been analyzed to yield the transverse and longitudinal optical-phonon frequencies near Γ, the high- and low-frequency dielectric constants, and an "ionicity" parameter. The ultraviolet dispersion has been correlated with single-electron interband transitions and many-body excitations. In addition to the room-temperature reflectance measurements, transmission data are reported over the range 0.04–2.8 eV down to 80 °K. In this energy range no exchange-related structure was detected. The Néel temperature was obtained from specific-heat measurements and confirmed by an independent optical technique. The value obtained 247 °K agrees with a previous determination. The results of this work are compared in detail with earlier work on MnO and MnS.

I. INTRODUCTION

The transition-metal (iron-group) chalcogenides display a large variety of optical, magnetic, and transport properties. These compounds have excited considerable interest, in part, as a consequence of this diversity. The elucidation of the electronic structure of these materials, particularly the nature of the states occupied by the *d* electrons, has been the principal effort. The present work is concerned primarily with MnSe and secondarily with two of the other insulating antiferromagnetic manganese chalcogenides, MnO and MnS. All three have sodium-chloride–structured phases with the lattice constant and magnetic exchange strength increasing as the atomic number of the chalcogenide ion increases. The optical and transport properties of MnO[1,2] and expecially of MnS[3] are partially known. Partial information is also available on the transport properties of MnSe.[4,5] The measurements presented in this paper provide optical data complementary to those previously obtained on MnO and MnS, and it was hoped that a detailed intercomparison might yield valuable clues in the interpretation of the optical and transport properties of the manganese chalcogenides. The information presented here will also be of use in interpreting the optical properties of other related insulating antiferromagnetic compounds, e.g., NiO and CoO. All of these materials have remarkably similar reflectance spectra. It seems possible that a single model with minor variations could be used to describe the optical properties of the insulating antiferromagnetic compounds MnO, MnS, MnSe, NiO, CoO, and, perhaps, other similar compounds as well.

II. SAMPLE PREPARATION AND GENERAL EXPERIMENTAL CONSIDERATIONS

MnSe crystallizes in three forms.[6] The α form, which has the NaCl structure, is the only one considered in this work. Bulk material was synthesized by a variation of the halide transport technique of Shäfer.[7,8] Stoichiometric amounts of high-purity Mn metal (99.9%)[9] and elemental Se (99.999+%)[10] were reacted at 900 °C in an evacuated quartz tube using resublimed I_2 as a catalyst. In a temperature gradient, transport would occur from the hot end to the cold end. The transported material was then baked out *in vacuo* at 1000 °C for about 20 hours. However, the resulting crystals, which display prominent (1, 1, 1) faces (octahedral habit), are of very poor quality due to etching and parallel growth. Material produced in this manner has been reported to be stoichiometric within the error limit 0.5%.[11] Oxygen content by neutron activation analysis[12] on a typical batch was 400 ppm. The lattice constant of the α-MnSe produced by this method is 5.461 Å and agrees with the value reported by Wiedemeier and Goyette.[11] Most of the optical measurements reported here were accomplished on films produced by flash sublimation.[13] This technique is required as the *in vacuo* sublimation of MnSe results in decomposition, i.e., the partial pressure of MnSe molecules is negligibly small above 1100 °C.[11]

Numerous substrate materials have been used, including single-crystal cleaved plates of MgO, CaF_2, NaCl, and also polished soft glass and fused quartz plates. At substrate temperatures above 250 °C epitaxy has been observed on all the above fcc materials. No epitaxial films examined showed Debye rings in the Laue x-ray diffraction photographs, and hence, were considered single crystals. The lattice constant of these films is in excellent agreement with the lattice constant measured on bulk material. The films were oriented so that their prominent face was the same as the cleavage plane of the substrate [i.e., (111) on CaF_2 and

(100) on NaCl and MgO]. On soft glass and fused quartz, of course, no epitaxy was possible, but lateral crystallization takes place, resulting in a very smooth, uniform polycrystalline film.

All sublimed films were produced in a standard vacuum evaporation system using a Veeco 2P2AB diffusion pump followed by a water-cooled baffle and liquid nitrogen trap. The maximum allowable distance from source to substrate was about 10 in., but virtually all films were produced at a distance of about 4 in. The base pressure of this system was about 1×10^{-7} Torr and during sublimation the pressure would rise to 10^{-6} Torr; however, the very high sublimation rates used (~ 500 Å/sec) greatly reduced contamination by the residual gas in the system. Epitaxial single crystals were used for transmission studies near the absorption edge. Unfortunately, for vacuum ultraviolet reflectance measurements, the surface of the epitaxial film samples was, in general, too rough and irregular due to imperfection in the cleaved surface, especially with MgO. Hence, all quantitative ultraviolet reflectance data reported in this work was obtained from polycrystalline films on smooth polished glass substrates produced by flash sublimation or by the following alternate technique.

If Mn metal is sublimed at a very rapid rate at 1000 °C from either a carbon or tantalum source onto a smooth glass substrate held at 250 °C, a mirror with a near perfect surface results.[14] This metallic film is then reacted rapidly, either directly with elemental selenium in a closed evacuated quartz tube, or reacted in a stream of ultrapure H_2 and H_2Se. The reaction, in either case, proceeds rapidly at a temperature of 250 °C.

The surface-smoothness requirements in the far infrared are relaxed in the present case. Hence, samples that were carefully polished mechanically were entirely adequate for studies of the reststrahl region. Bulk MnSe, prepared as already outlined, was finely ground in an argon-filled glove bag, and pressed into a 13-mm-diam pill about 1.5 mm thick under a force of 17 tons. This pill was then sintered *in vacuo* at 1000 °C for 20 h. The resulting pill was mechanically quite strong and had a density of about 95% of the single-crystal density. Polishing was accomplished by a standard technique using a small pitch lap and methyl alcohol as a dispersing agent.

Table I gives a summary of the various sample types employed in the transmission studies and the reflectance measurements in the infrared and ultraviolet regions.

TABLE I. Summary of sample types employed in the optical investigations.

Region	Sample type	Measurement
200–2.4 μ (0.006–0.5 eV)	Polished pressed pill	Normal incidence reflectance study of the reststrahl absorption (Sec. III).
17 000–4600 Å (0.7–2.6 eV)	Thick polycrystalline films on smooth glass substrates	Normal incidence reflectance in the transparent region (Secs. III and IV).
17 000–4600 Å (0.7–2.6 eV)	Epitaxial single-crystal films on single-crystal substrates	Normal incidence transmission studies of crystal field spectra (Sec. IV).
4600–800 Å (2.6–16 eV)	Thin polycrystalline films on smooth glass substrates	Normal incidence reflectance studies of interband and collective electron effects (Sec. V).

III. INFRARED OPTICAL PROPERTIES

The infrared absorption spectra of polar insulating crystals is dominated by the resonant lattice absorption (reststrahl). This absorption, at ω_T, corresponds to the creation of a transverse optical phonon of very small wave vector by the incoming photon. Classical harmonic-oscillator dispersion theory has been extensively applied in the analysis of experimental spectra.[15,16] However, if the reststrahl spectra displays prominent second-order (multiphonon) absorption, it is much more convenient to obtain the optical constants in this region by a Kramers-Kronig phase-shift dispersion analysis.[17]

It is usually more convenient to display infrared spectra on a wavelength scale. Also, if an evenly spaced integration grid is employed, as is required for a Simpson's rule integration, it is of considerable advantage to perform the integration on a wavelength scale. The standard Kramers-Kronig dispersion integral[18] with the change of variable $\omega = 2\pi c/\lambda$ differs from the original form only by a change in sign. Thus we have

$$\theta(\omega) = -\frac{2\omega}{\pi}\int_0^\infty \ln\left(\frac{r(\omega')}{r(\omega)}\right)\frac{1}{\omega'^2-\omega^2}\,d\omega', \tag{1}$$

$$\theta(\lambda) = \frac{2\lambda}{\pi}\int_0^\infty \ln\left(\frac{r(\lambda')}{r(\lambda)}\right)\frac{1}{\lambda'^2-\lambda^2}\,d\lambda', \tag{2}$$

where $R(\omega) = \tilde{r}^*(\omega)\tilde{r}(\omega)$ and $\ln\tilde{r}(\omega) = \ln r(\omega) + i\theta(\omega)$. This form of the dispersion integral (either wavelength or frequency integration) does not explicitly contain the principal value, and so is much more accurate and expeditious than the other commonly used forms for numerical calculation. In polar insulating compounds, the reststrahl and interband absorptions are well separated in energy. Hence, analysis of one region can be made independently of the other with high accuracy, since the oscillator strength of interband transitions in the reststrahl region is negligible, and vice versa.

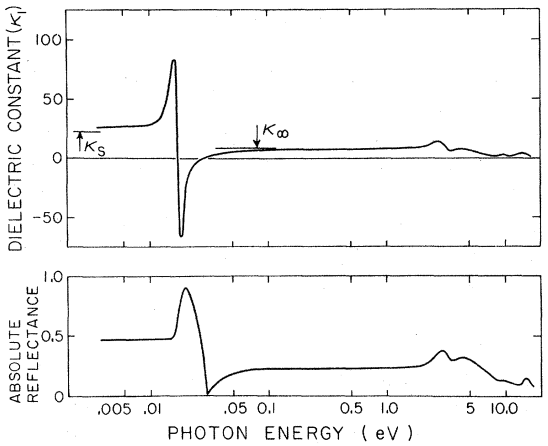

FIG. 1. Spectral variation of the reflectance and the real part of the dielectric constant over the range in energy 0.006–16 eV as determined in this work for the polar insulator MnSe.

Of course, in order to implement the dispersion analysis, some sort of extrapolation is necessary on both ends of the data interval, as in the case of dispersion analysis of high-energy reflectance data. If the data range, which extends from λ_{min} to λ_{max}, is such that the reflectance is constant at each end of the data interval, the reflectance may be simply extrapolated as a constant.[19] For example, the contribution to the phase for $\lambda < \lambda_{min}$ is

$$\theta_1(\lambda) = \frac{2\lambda}{\pi}\int_0^{\lambda_{min}} \ln\left(\frac{r(\lambda')}{r(\lambda)}\right)\frac{1}{\lambda'^2-\lambda^2}\,d\lambda' \tag{3}$$

$$= \frac{1}{\pi}\ln\left(\frac{r(\lambda_{min})}{r(\lambda)}\right)\ln\left|\frac{\lambda_{min}-\lambda}{\lambda_{min}+\lambda}\right| . \tag{4}$$

Experimentally, for most polar compounds, it is possible to extend the data interval on the small-wavelength end as far as $\lambda/\lambda_T \sim 0.01$ before the reflectance is disturbed by the higher-energy interband structure (see Fig. 1). Hence, the constant reflectance extrapolation in this case is very well justified. However, on the large-wavelength end, it is experimentally difficult to get accurate reflectance data beyond $\lambda/\lambda_T \sim 3$. If λ_{max} is only on the order of $3\lambda_T$, the assumption of a long-wavelength constant reflectance extrapolation will lead to a large error in the reflectance phase at long wavelength. This will, in turn, lead to large errors in the optical constants in this region. The solution is to adopt an extrapolation derived from the classical lattice dispersion model.[20] For $\lambda/\lambda_T \gg 1$, k is nearly zero, and so $r \cong (n-1)/(n+1)$. By expanding the classical dispersion reflectance result, we have

$$r(\lambda') = r_s + C(\lambda_T/\lambda')^2 , \tag{5}$$

where

$$r_s = (n_s-1)/(n_s+1), \quad C = (n_s^2 - n_\infty^2)/n_s(n_s+1)^2 .$$

The constants n_s and n_∞ are, respectively, the static and high-frequency indices of refraction. The long-wavelength contribution to the phase is then

$$\theta_3(\lambda) = \frac{2\lambda}{\pi}\int_{\lambda_{max}}^{\infty} \ln\left(\frac{r(\lambda')}{r(\lambda)}\right)\frac{1}{\lambda'^2-\lambda^2}\,d\lambda' \tag{6}$$

$$= -\frac{1}{\pi}\ln\left(\frac{r_s}{r(\lambda)}\right)\ln\left|\frac{\lambda_{max}-\lambda}{\lambda_{max}+\lambda}\right| - \left(\frac{C\lambda_t^2}{\pi r_s}\right) \times\left(\frac{2}{\lambda\lambda_{max}} + \frac{1}{\lambda^2}\ln\left|\frac{\lambda_{max}-\lambda}{\lambda_{max}+\lambda}\right|\right) . \tag{7}$$

The complete expression for the phase is then given by the sum of $\theta_1(\lambda)$, $\theta_3(\lambda)$, and the numerical integration of the dispersion integral over the data interval $\theta_2(\lambda)$. The optical constants n and k are then easily computed from the phase and reflectance amplitude. For completeness, the complex index of refraction ($\tilde{N} = n + ik$) and the complex dielectric constant ($\tilde{\kappa} = \kappa_1 + i\kappa_2$) are related according to $\kappa_1 = n^2 - k^2$, and $\kappa_2 = 2nk$. Although the large-wavelength extrapolation tail discussed above is rigorously valid only for $\lambda/\lambda_T \gg 1$, computation on synthetic harmonic-oscillator reflectance data has shown that for optical constants and damping similar to those in the present case, the expression gives accurate results even for $\lambda/\lambda_T \sim 2$.

All data were taken point by point using a Perkin Elmer model 301 far-infrared spectrophotometer (see Fig. 2). The Perkin Elmer reflectance attachment for this instrument was modified so that either the sample, an aluminum mirror reflectance standard, or a zero reflectance standard could be rotated into the beam without breaking the dry N_2 purge. Over most of the data range the apparent scatter in the data is about 0.005 reflectance units or less. The absolute accuracy of the measured reflectance is difficult to assess. The fact that a polished pressed pill was used probably affects the data only at the smallest wavelengths and would tend to depress the reflectance due to diffuse scattering. However, one must treat the results obtained from such samples with some caution as it has been demonstrated that a rough surface can introduce spurious structure into the reststrahl reflectance.[21] The subsidiary structure shown in the MnSe reststrahl of this work is thought not to be due to this cause, but rather to multiphonon absorption. This conclusion is based on the quantitative observation of the same reflectance features in not only the two samples reported here, but also in other unreported samples. In any case, the subsidiary structure is small and has no consequence for the analysis presented. One sample (No. 2) was composed of material supplied by Electronic Space Products[22] and

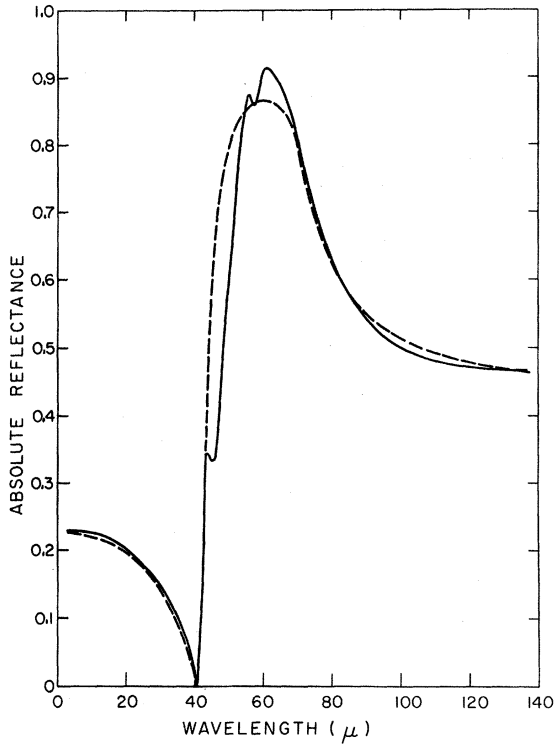

FIG. 2. Experimental MnSe reststrahl reflectance (full curve) together with harmonic-oscillator reflectance (dashed curve). Harmonic-oscillator-model parameters $\kappa_s = 22.6$, $\kappa_\infty = 8.0$, $\lambda_T = 71.0\,\mu$, and $\gamma/\omega_T = 0.106$.

was claimed to be 99.996% pure. The other pill (No. 3) was composed of material prepared by I_2 catalysis as described earlier. Pill No. 2 was run with an aluminum reference mirror produced in this laboratory. Aluminum, 99.99% pure, was evaporated from a multistrand tungsten wire source onto a microscope slide substrate at 10^{-5} Torr. Pill No. 3 was run against a mirror supplied by Dr. H. E. Bennett of the Michelson Laboratory, China Lake, California. For some unknown reason, pill No. 3 is considerably more dense than pill No. 2, and the polished surface is more nearly perfect. Accordingly, only reflectance results for pill No. 3 were analyzed in detail, although the experimental reflectances on both pills were in agreement to within 0.04 reflectance units at all points. Over most of the data range the agreement is much better, the difference being less than 0.01 units.

From a dispersion analysis of the reststrahl resonance, one obtains the high- and low-frequency dielectric constants κ_∞ and κ_s directly as the limiting values of κ_1. The transverse optical mode frequency ω_T is given approximately by the position of the main peak in κ_2 (see Fig. 3). A more precise value can be computed from the following relationship obtained from the classical dispersion model by setting the derivative $d\kappa_2/d\omega$ to zero:

$$\omega_0/\omega_T \cong 1 - \tfrac{1}{8}(\gamma/\omega_T)^2 \,. \tag{8}$$

The frequency ω_0 is the position of the maximum in κ_2, and γ is the phenomenological damping parameter. The damping near ω_T can be obtained easily by considering κ_2 at ω_T. We have

$$\kappa_2(\omega_T) = \frac{\kappa_s - \kappa_\infty}{\gamma(\omega_T)/\omega_T} \,. \tag{9}$$

If γ/ω_T is small, very little error will be introduced in setting $\kappa_2(\omega_T) = \kappa_2(\omega_0)$, so we have

$$\gamma(\omega_T)/\omega_T \cong (\kappa_s - \kappa_\infty)/\kappa_2(\omega_0) \,. \tag{10}$$

The longitudinal optical mode wavelength at Γ was computed from the Lyddane-Sachs-Teller relationship.[23] The value obtained, 42.2 μ, is in excellent agreement with the position of the zero of κ_1 at 42.3 μ. This is, of course, a consequence of negligible damping in this region. In addition to the parameters of the classical oscillator, we can also compute the total electronic polarizability α, the bulk modulus B, and an "ionicity" parameter e_T^*.[24] Table II gives the computed reststrahl parameters. The values of crystal electronic polarizabilites given by Tessman, Kahn, and Shockley[25] are not entirely self-consistent due to the dependence of the polarizability on environment. From the Tessman, Kahn, and Shockley tables, one obtains a range of polarizability for Se^{2-} from 6.0 to 7.5 $\times 10^{-24}$ cm^3. The value of α for MnSe (6.79 $\times 10^{-24}$ cm^3) obtained in this work is reasonable if one assumes that the polarizabilities of Mn^{2+} and Se^{2-} are additive, since the polarizability of Mn^{2+} must be quite small.[26] The departure of the effective-charge ratio from unity is considerable, even for the alkali halides, which are considered highly ionic. In general, this departure has to be accounted for in some manner other than simply reduced ionicity. The shell model presented by Dick and Overhauser[27] partially accounts for this discrepancy by including polarization mechanisms absent in the simple model. However, in the present case one must assume that the relatively large departure from unity is due, in part, to the presence of covalent bonding. A recent series of papers by Phillips[28] discusses this problem. In examining

TABLE II. Parameters of the room-temperature first-order reststrahl absorption in MnSe.

κ_s	22.6
κ_∞	8.0
λ_T	71.0 μ (141 cm^{-1})
λ_L	42.2 μ (237 cm^{-1})
$\gamma(\omega_T)/\omega_T$	0.106
$e_T^*/2e$	0.42
α	6.79×10^{-24} cm^3
B	5.69×10^{11} dyn/cm^2

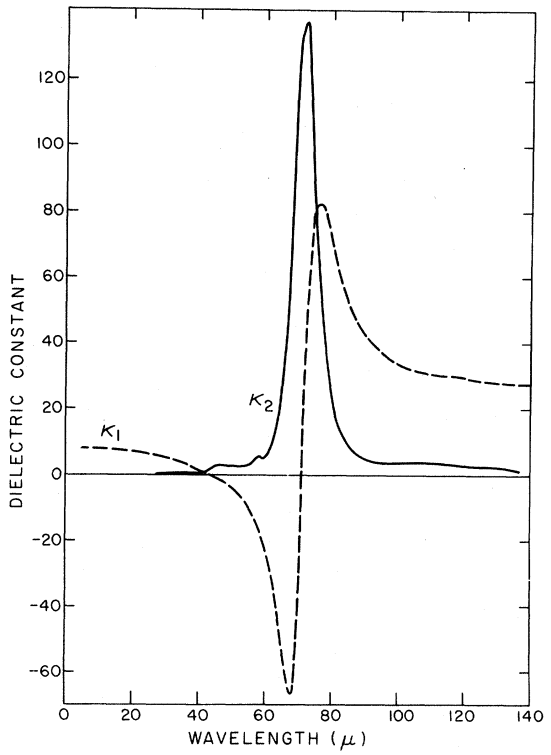

FIG. 3. Spectral dependence of the real and imaginary parts of the dielectric constant in the reststrahl region obtained by a phase-shift analysis of the reflectance data.

calculated and measured bulk moduli of a large number of compounds[24] it seems unlikely that the error in the calculated value presented here will be greater than 50%.

In addition to room-temperature near-normal-incidence reflectance data, transmission and reflectance data were taken down to 80 °K over the range 15–60 μ. Below the critical temperature, all magnetically ordered materials should display additional absorption structure due to the interaction, either directly or indirectly (via phonon participation), of the radiation field with the magnon modes of the crystal.[29–31] Calculations based on the model proposed by Mizuno and Koide[30] for the spin-dependent absorption in NiO give the position of the main spin-dependent absorption in MnSe at 21.5 μ, assuming a Néel temperature of 247 °K.[32,33] At T = 100 °K, over the region 15–40 μ, no change in reflectance larger than the signal noise (~1% of the reflected signal) could be seen. Over this region $k \lesssim 0.1$ and it is estimated that an absorption as small as 100 cm^{-1} could have been detected. Above about 45 μ, the reflectance curve is steepened considerably ($R_{100\,°K}/R_{300\,°K} = 2.1$ at 46.5 μ), which is due to a shift in the second-order absorption towards shorter wavelength. The absorption structure appearing just before 40 μ (see Fig. 4) is unshifted at low temperatures. This structure probably should be considered spurious, and due to relatively large errors occurring in the reflectance near the reflectance minimum. An additional very weak and broad absorption in the room-temperature spectra on the other side of the main dispersion at 95 cm^{-1} (position in κ_2) occurs at an energy corresponding to the energy difference of the TO and LO mode at Γ, and, hence, is tentatively identified as the difference band $LO_\Gamma - TO_\Gamma$.

Since the spin-dependent absorption reported in NiO[29] is only 30 cm^{-1}, reflectance techniques lack sufficient sensitivity to detect the corresponding absorption in MnSe if it is as small. Transmission measurements performed on a single-crystal platelet grown by the I_2 transport technique at 80 °K, and with a sensitivity of 2 cm^{-1}, failed to show any wavelength-dependent absorption over the region 15–30 μ. However, a broad (wavelength-independent) "absorption" of ~10 cm^{-1} was observed. The temperature dependence of this absorption is shown in Fig. 5. This "absorption" is due to the interaction of the optically active MnSe sample in its antiferromagnetic state[34] with the reflectometer instrumental polarization. Hence, this experiment provides an independent optical measurement of T_N, which is in agreement with the previously assumed

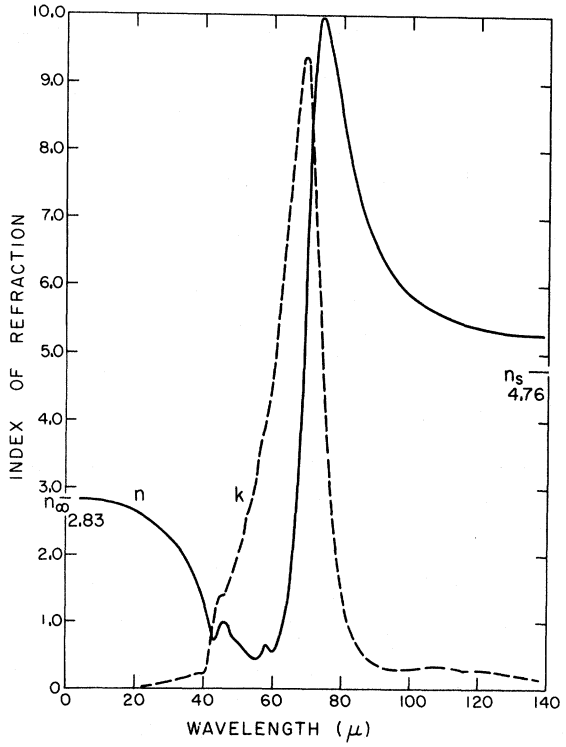

FIG. 4. Spectral dependence of the real and imaginary parts of the index of refraction in the reststrahl region obtained by a phase-shift analysis of the reflectance data.

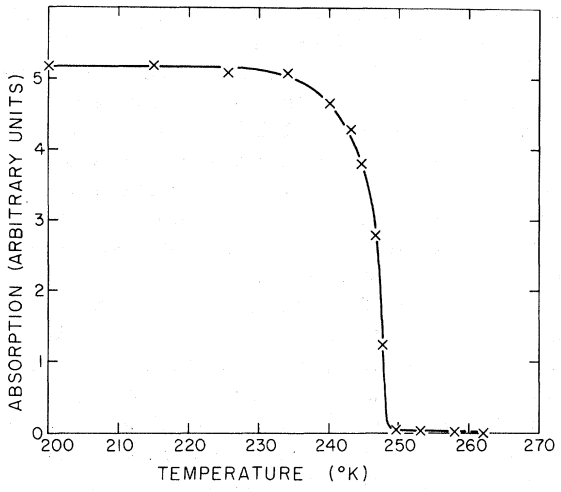

FIG. 5. Temperature dependence of the apparent absorption in a MnSe single crystal as a consequence of optical activity.

(specific-heat) value.

IV. FUNDAMENTAL ABSORPTION EDGE, EXCITONS, AND CRYSTAL FIELD EFFECTS

Many transition-metal compounds and aqueous solutions of transition-metal ions are brightly colored due to sharply defined "windows" in the transmission spectra. The absorption structure responsible can be quantitatively treated by ligand field theory, as developed largely by Tanabe and Sugano[35] and Orgel.[36] As originally developed, the theory was intended to apply to transition-metal ions in dilute concentration (hydrated ions in aqueous solution or as substitutional impurities in a host crystal lattice). More recently, however, the theory has been applied to systems of high-ion concentration, e.g., transition-metal compounds. The experimental spectra of a large number of transition-metal compounds are in reasonable quantitative agreement with predictions of ligand field theory.

Accordingly, one ascribes the observed "crystal field" optical absorption in Mn^{2+} to transitions between the ground-state ^6S and the higher-lying excited-state levels derived from the crystal-field-split ^4G, ^4P, ... states of the free ion. Such transitions will be doubly unallowed (parity and spin) for dipole radiation, and hence, coupling to some intermediate state is required to give a nonzero transition probability. Optical absorption measurements on the system $Ni_xMg_{(1-x)}O$ indicate that there is essentially no overlap between d electrons of adjacent sites.[37] Hence, the basic assumption of ligand field theory is essentially fulfilled in NiO. However, the d electrons are not strictly localized (i.e., core electrons) as evidenced by the presence of an exchange field and antiferromagnetic order below T_N. This extremely important result is immediately applicable to other similar compounds, e.g., MnO, MnS, and MnSe. The quantitative success of ligand field theory implies that the $3d$ electrons in these compounds are highly localized. The absorption structure appearing in Fig. 6 is unambiguously identified as crystal field absorption by detailed comparison with the corresponding structure in MnO and MnS.[1,2,3] This absorption is superimposed on a steep absorption edge which rises to $\sim 10^6$ cm^{-1}. A similar association is present in MnO and MnS, however, the absorption edge shifts to lower energy as the chalcogenide ion becomes heavier while the crystal field structure remains more or less stationary. Hence, in MnSe the crystal field structure is "buried" much deeper in the edge than is the case for MnO.

An ordinary band calculation cannot accurately describe the highly correlated many-body states occupied by the d electrons. However, the electron states of the crystal responsible for the bonding [arising from the transition-metal 4s orbitals and chalcogenide (2, 3, 4) p orbitals] should be described in the ordinary one-electron band formalism. The nature of the absorption edge in the manganese chalcogenides remains uncertain even

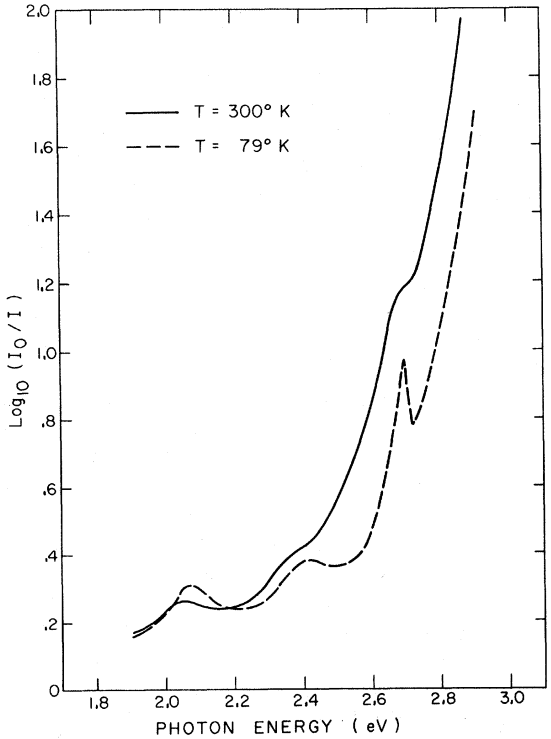

FIG. 6. Spectral dependence of the absorbance of a MnSe single-crystal film in the vicinity of the fundamental absorption edge, showing the "crystal-field-splitting" structure.

after extensive work, both theoretical and experimental. Recent band calculations place the $3d^5$ states between the broad (2, 3, 4) p "valence" and the $4s$ "conduction" bands.[38] This is also suggested by a simple ionic energy-band calculation.[39] In NiO and CoO this ordering is also confirmed by photoemission experiments.[40,41] If we assume this ordering, the edge could either be a consequence of $p \rightarrow d$ or $d \rightarrow s$ transitions. The latter excitation is not electric dipole allowed, but there may be sufficient state mixing so that the dipole selection rules are broken down. There is indirect evidence for the participation of the (3, 4) p electrons in the absorption edge of MnS and MnSe from an analysis using a dispersion model proposed by Wemple and DiDomenico.[42] In this model, the dispersion in the real part of the dielectric constant κ_1 is represented by a Sellmeier oscillator for $E < E_g$. Hence, we write

$$\kappa_1(E) - 1 = \mathfrak{F}/(E_0^2 - E^2) \ . \tag{11}$$

This simple relationship accurately describes the low-energy dispersion in a large number of ionic and covalent solids, including MnS and MnSe. Unfortunately, dielectric dispersion data in this region is not available for MnO. Wemple and DiDomenico define a dispersion energy $E_d \equiv \mathfrak{F}/E_0$. For most of the compounds studied, this quantity has the property of obeying the empirical relationship

$$E_d \cong 0.3 N_c Z N_e \ , \tag{12}$$

where N_c is the coordination number (6 for the octahedral coordination of the NaCl structure), Z is the anion valence, and N_e is the effective number of valence electrons per anion. For MnS and MnSe one calculates $E_d = 30.3$ and 33.2 eV, respectively. N_e is then approximately 8, which corresponds to the occupation of a saturated (s-p) valence band. One, therefore, has evidence of participation of the (3, 4) p electrons in the edge absorption. However, this evidence must be viewed with some caution since the same analysis, when applied to the europium chalcogenides, yields anomalous results.[42] This is apparently a consequence of the participation of the $4f$ electrons in the edge absorption and the small oscillator strength associated with their excitation.

The results of Fig. 6 were obtained from a single-crystal film 0.98 μ in thickness, deposited on a (1, 1, 1) cleaved surface of a CaF_2 single crystal. All transmission measurements were accomplished on a Cary 14R spectrophotometer. The sample thickness was determined from the positions of successive minima and maxima in the interference structure appearing in the transmission spectra. The correct fringe order was assigned by plotting fringe order vs $1/\lambda$. The optical thickness nd is then determined from the slope of this plot. The thickness can then be calculated using the index of refraction computed from the infrared reflectance data of Sec. III. A very careful examination of the transmission spectra of this sample and several other samples as thin as 0.2 μ, at temperatures down to 10 °K, failed to show any structure not shown in Fig. 6. At liquid helium temperatures the crystal field peak at 2.7 eV shows a hint of additional structure, but nothing is actually resolved. The temperature shift in the absorption edge from 300 to 80 °K is seen from Fig. 6 to be approximately 0.08 eV towards the violet. The corresponding shifts in MnO and MnS are, respectively, 0.1 and 0.3 eV.[2,3] As is suggested in Sec. V, the actual absorption edge is possibly due to an exciton. Hence, the relatively large differences in observed shifts in the manganese chalcogenides may be the result of changes in the exciton absorption rather than in shifts of the band edges themselves.

The temperature dependence of the crystal field absorption energies has been related to the temperature dependence of the exchange.[2,3] In the present case, a rather large exchange shift was expected as a consequence of the relatively high Néel temperature (MnO, 120 °K; MnS, 152 °K; MnSe, 247 °K). The crystal field absorption in MnSe is very nearly at the same energy as in MnO and MnS. However, the absorption edge is shifted approximately 2 eV towards the red in comparison with MnS. Consequently, the sharpest peak (at 2.7 eV) is situated very high on the absorption edge, and at room temperature appears only as a shoulder. An actual peak is not resolved until the sample is cooled to 200 °K. The shift in wavelength from the position of this peak at 200 to 10 °K is less than the limit of resolution (5 Å). Hence, it is not possible to determine even the direction of the shift. From Fig. 6 it appears that the peak at 2.5 eV is shifted ~0.01 eV towards the violet at 79 °K. This is perhaps only an apparent shift, since the original spectra included interference structure which was removed mathematically. This correction quite conceivably could be in error by the amount of the apparent shift, due to the very broad nature of both the lower-energy crystal field peaks and the interference structure itself.

V. ULTRAVIOLET OPTICAL PROPERTIES AND ELECTRON ENERGY-BAND STRUCTURE

The highly dispersive interband transitions associated with the fundamental absorption edge and beyond in the ultraviolet are most easily explored by reflectance techniques.[43,44] For allowed transitions, the absorption will rise to ~ 10^6 cm^{-1} (see Fig. 7). As in the case of reststrahl absorption, the use of thin film transmission measurements is limited by problems of nonbulk effects and also by a lack of

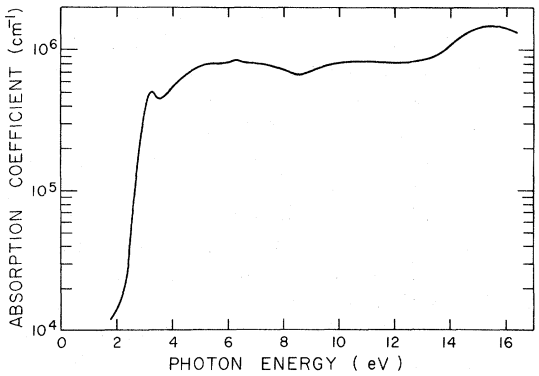

FIG. 7. Spectral dependence of the absorption coefficient.

suitable transparent substrates below 1000 Å. As in the reststrahl absorption, the single-angle reflectance technique was chosen, primarily because of intensity restrictions imposed by the small samples employed. Surface quality for reflectance measurements in the vacuum ultraviolet is particularly critical in regard to chemical purity, crystalline perfection, and surface roughness.[45,46] Only samples of the highest quality will possess a quantitative specular reflectance. For MnSe there is the added difficulty of chemical instability in moist air. This is responsible, undoubtedly, for most of the variation in reflectance results from sample to sample, especially in the early samples. This problem ideally would be circumvented by *in situ* production of the reflectance surface in the high vacuum of the ultraviolet monochromator. The sample surface also was observed to deteriorate under the action of the hydrogen gas in the reflectometer when the Hinteregger discharge lamp was run in the windowless configuration. This photochemical reaction has also been reported in the lead chalcogenides,[44] but in the present case it does not appear to be serious, since the time required for appreciable change (0.005 reflectance units) in the 1600–800-Å region appears to be many hours.

It should be emphasized that although large quantitative variations (~0.1 reflectance units) were observed between various samples, the details of the reflectance spectrum reported in Fig. 8 have been corroborated by the data obtained from several dozen samples. These samples have included polished pressed pills, polished single-crystal samples, epitaxial single-crystal films, and polycrystalline films. In general, the reflectance results of polished samples display structure very similar to the results of the better samples, but "blurred out" and in the poorest samples shifted in energy by the effect of the distrubed surface. The epitaxial films suffered considerably from effects of surface roughness, although most samples, up to 4 to 5 eV, give results in substantial agreement with the polycrystalline film samples. The polycrystalline films deposited on smooth soft glass or fused quartz substrates displayed uniformly greater reflectance in all regions and the data more consistent than from epitaxial single-crystal films. This is a result, presumably, of the much smoother surface of the polycrystalline films. Beyond 4 eV, the reflectance variation between several samples was ~0.04 reflectance units out to 12 eV and somewhat greater beyond this point. The peak at 3 eV, however, displayed a large variation in intensity from sample to sample. This phenomenon was also observed in the corresponding peak in MnS.[47] In the transparent region (0.05–2.5 eV) relatively thick samples are required ($d > 50\ \mu$) unless a thin-film reflectance analysis is used. In the present work, thick polycrystalline films on glass substrates were used. In general, the surface smoothness of vacuum deposited films decrease as the film thickness increases. Consequently, the absorption edge reflectance in MnSe has a relatively large uncertainty.

All measurements reported here in the range 2.5–16 eV were accomplished on a McPherson model 235, 0.5-m Seya-Namioka vacuum ultraviolet monochromator. The dispersing element was a 600 lines/mm grating blazed at 3500 Å. The grating was used in first order only. Unwanted higher-order diffracted light was removed by soft glass or quartz filters positioned just after the exit slit. A 1-kW quartz-iodine lamp was used as a source from 6000–3800 Å (2–3.3 eV), and a 1-kW Hinteregger-type discharge lamp, supplied by McPherson, was employed from 3800–700 Å (3.3–17.2 eV). The hydrogen continuum was utilized up to 14.4 eV, and, above this energy, reflectance points were obtained at 16.7 and 17.2 eV using argon gas at very low pressure. An EMI 9514S photomultiplier detector mounted externally to the sample compartment utilized a conventional silvered Pyrex light pipe arrangement. Below 3800 Å, a sodium salicylate phosphor coat was applied to the end of the light pipe from an ethyl alcohol solution. The reflec-

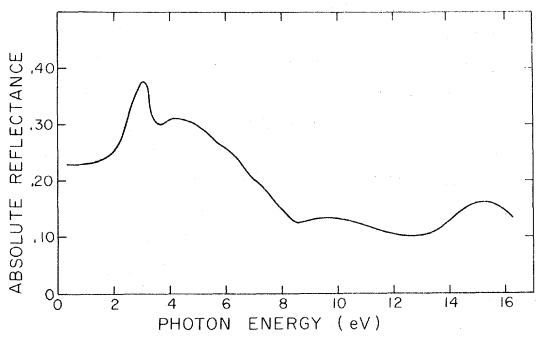

FIG. 8. Spectral dependence of the vacuum ultraviolet near-normal-incidence reflectance of MnSe.

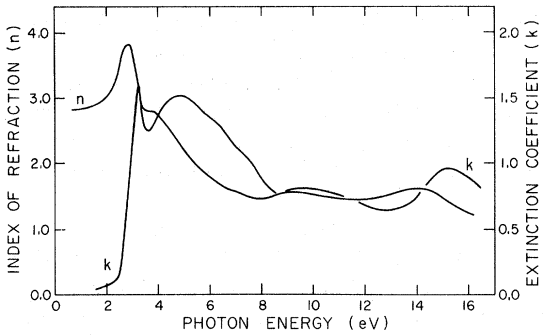

FIG. 9. Spectral dependence of the real and imaginary parts of the index of refraction determined by a phase-shift analysis of the reflectance data.

tance attachment was so constructed that by rotating the top turret either the full beam or the reflected beam could be received, thus providing an absolute near-normal-incidence reflectance measurement. The actual angle of incidence was 11°.

The ultraviolet optical constants were obtained from a Kramers-Kronig phase-shift dispersion analysis of the near-normal-incidence reflectance data. The phase contribution of the region less than 0.1 eV was obtained by a constant reflectance extrapolation, in which we have

$$r(E) = r(0) = \frac{n_\infty - 1}{n_\infty + 1} \tag{13}$$

This, of course, neglects the reststrahl absorption and is justified by the arguments presented in Sec. III. The phase contribution from this region $\theta_1(E)$ is given by Eq. 4 with a change of sign and by replacing λ by E. The contribution over the data interval $\theta_2(E)$ is obtained by numerical integration of Eq. 1. The contribution of the high-energy region was obtained by both a modified Roessler extrapolation[48] and also a power-law extrapolation of adjustable exponent.[18] For both extrapolations, the adjustable parameter of the extrapolation was used to force the phase at some energy on the absorption edge to assume a value so that the computed extinction coefficient at that energy was identical with the measured value (see Fig. 9). Hence, the computed phase at low energy is nearly identical for both extrapolation schemes. The two methods differ significantly only at high energy where, in general, the Roessler extrapolation yields a phase which is too large. In the present case the Roessler extrapolation yields a phase at 16 eV which actually exceeds π. This is a consequence of the overestimate of the actual high-energy reflectance by the Roessler extrapolation which is essentially a constant reflectance extrapolation. The optical constants reported here were obtained by a power-law extrapolation. Computation on reflectance data obtained from a variety of samples has revealed that although there are large differences in the computed optical constants especially at high energy, the peak positions of all structures are in agreement to 0.15 eV or less. Hence, it is felt that the ultraviolet reflectance data presented is adequate for the purposes of this paper.

The composite reflectance data of Fig. 8 was obtained as follows: The reflectance from 0.1 to 3.0 eV is the average of results obtained on two thick polycrystalline samples produced by sublimation of manganese onto a smooth soft glass substrate and subsequent reaction with H_2Se. The data from 3.0 to 4.0 eV is the result of measurements on a single thin polycrystalline sample produced in an identical manner. The data from 4.0 to 16.0 eV was obtained from the average of three polycrystalline samples, one produced by the sublimation of manganese metal onto a smooth soft glass substrate and subsequent reaction with H_2Se and two samples produced by the flash sublimation of MnSe onto a similar substrate.

The optical constants obtained from these data will be discussed with particular attention to several newly recognized aspects and the inferences which can be made from them. Powell and Spicer have recently reviewed several possible absorption models for NiO.[41] The same models are directly applicable also to the manganese chalcogenides. A detailed comparison of the reported reflectance spectra of NiO, CoO,[41] MnS[3], and MnSe in the present work discloses a remarkable general similarity, except for differences in structure just after the initial peak.

Crucial to the interpretation of the optical results is the presence or absence of photoconductivity. Photoconductivity has been reported at the edge energy in MnO.[49] The same work also reports photoconductivity at the crystal field peak energies. It is certain that this latter photoconductivity, at least, is not a simple type. Unreported photoconductivity measurements on MnS single-crystal platelets yielded only negative results over the range 2–6 eV.[50] The most recent photoconductivity data on NiO indicates similar results over the range 4–7 eV.[40] It is concluded that in NiO and MnS (and, by inference, also MnSe and MnO) the optical excitations over the region from the absorption edge to the first reflectance minimum are localized. Many-body effects are probably important in this region.[51] We suggested in Sec. IV that the edge absorption was a consequence of excitation of the chalcogenide (2, 3, 4) p electrons. Since the hole that was left in the broad p band after excitation would lead to a conducting state, contrary to photoconductivity results, the excitation cannot be an ordinary band transition. The possibility that the edge absorption is a "charge transfer excitation" has been previous-

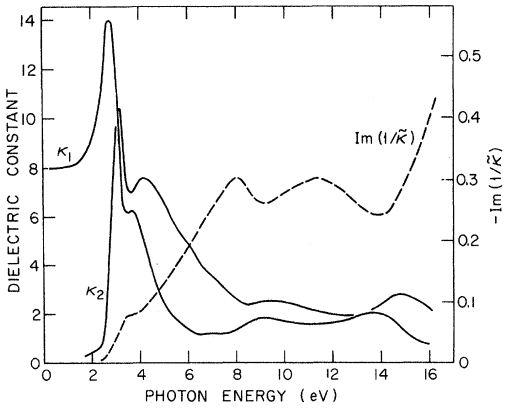

FIG. 10. Spectral dependence of the real and imaginary parts of the dielectric constant and the optical electron energy-loss function $-\mathrm{Im}(1/\tilde{\kappa})$ determined by a phase-shift analysis of the reflectance data.

ly suggested for NiO.[29] In this model an electron is removed from a chalcogenide anion (2, 3, 4) p orbital and placed in a $3d$ or $4s$ orbital of neighboring transition-metal cation. In either, the "transfer exciton" above or the other localized exciton model discussed briefly by Powell and Spicer,[41] the electron wave function is given in a tight-binding approach as a suitable linear combination of atomic wave functions.

Of course, it is possible that we are seeing d-electron excitation in the absorption edge region.[41,52] Further elucidation of whether d or p electrons are being excited in this region could come from an analysis of the volume plasma resonances present in all of these materials. The function $-\mathrm{Im}(1/\tilde{\kappa}) = \kappa_2/(\kappa_1^2+\kappa_2^2)$ is proportional to the characteristic energy loss for transmission of energetic electrons through thin films.[18,53] The electron energy-loss spectrum in such an experiment shows characteristic sharp absorption peaks corresponding to single-electron excitations and collective plasma oscillations. Collective plasma oscillations are conveniently described in terms of a frequency-dependent longitudinal dielectric constant.[54] However, in a cubic crystal in which the dielectric constant is a scalar, and in the limit of small wave vector, the longitudinal dielectric constant is identical with the transverse (optical) dielectric constant. Hence, one may compute an optical electron energy-loss function $-\mathrm{Im}(1/\tilde{\kappa})$ from the dielectric constants derived from the phase-shift analysis of the reflectance data.[55]

From an inspection of Fig. 10, peaks in the energy-loss function can also be clearly associated with "interband transitions." However, the two physical phenomena can be unambiguously separated by an inspection of the complex dielectric constant. In the region of a plasma resonance, both κ_1 and κ_2 will be small, and have, respectively, positive and negative slopes.[56] This situation is very much unlike that for interband absorption. Therefore, the peaks in $-\mathrm{Im}(1/\tilde{\kappa})$ at 8.1 and 11.5 eV are identified as representing collective plasma oscillations. The energy-loss function computed from the MnS data of Huffman and Wild[3] shows a single well-defined plasma resonance at 9.5 eV. Of course, these resonances are virtual, since it is not possible to excite a longitudinal plasma oscillation with plane wave electromagnetic radiation normally incident upon a smooth surface. It is obvious from an inspection of the complex dielectric constant near 8.1 and 11.5 eV in MnSe and 9.5 eV in MnS that these resonances are strongly screened and thus, are not free-electron-like. This results in a large depression of the resonance energy below its free-electron position. Wilson has studied phenomenologically the effect on a plasma resonance from a higher-energy interband transition and predicts qualitatively the shift to lower energy as seen here.[57] A similar large shift is also seen in the conduction-electron plasma resonance in Ag.[58] This effect may be very crudely accounted for by introducing a screened plasma frequency ω_p',[54,58] where

$$\omega_p'^2 = (n_{\mathrm{eff}}e^2/m\epsilon_0)\,(1+\delta\kappa_1)^{-1}\,. \tag{14}$$

In this expression n_{eff} is an effective electron concentration and $\delta\kappa_1$ is the contribution of the lower-lying electrons to the high-frequency dielectric constant at the screened plasma energy. In Fig. 11 we have plotted the contribution to the high-frequency dielectric constant in an energy range less than E, as computed from the sum rule

$$\kappa_{\mathrm{eff}}(E) = 1 + (2/\pi)\int_0^E [\kappa_2(E')/E']\,dE'\,. \tag{15}$$

The difference in the dielectric constant at some energy E and the asumptotic value $\kappa_\infty = 8.0$ is the contribution to the high-frequency dielectric con-

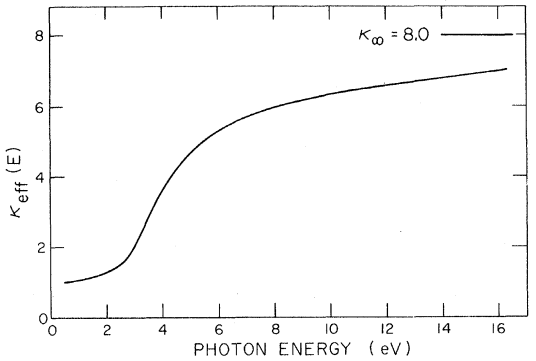

FIG. 11. Plot of the effective dielectric constant due to interband transitions occurring in the range of energy up to E.

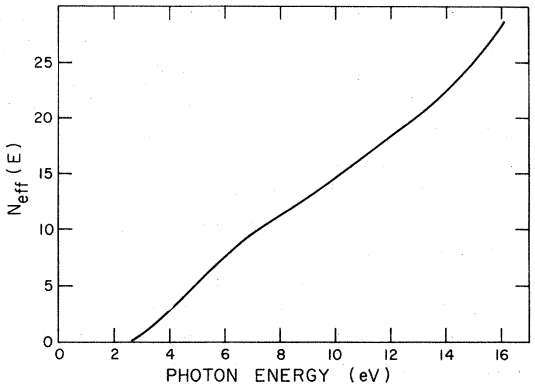

FIG. 12. Plot of the effective number of free electrons contributing to the optical constants in a range of energy less than E.

stant in the energy range above E, $\delta\kappa_1(E)$. Hence, the effective number of electrons participating in the collective plasma oscillation may be computed. For the 8.1-eV resonance in MnSe, one obtains $n_{eff} = 23.4$ electrons/unit cell and for the 9.5-eV resonance in MnS, one computes $n_{eff} = 17.2$ electrons/unit cell. These values for n_{eff} are reasonably close to the electron concentrations expected for *either* $4p^6$ or $3d^5$ excitation, 24 and 20 electrons/unit cell, respectively. Unfortunately, the crudeness of the analysis prevents a more quantitative comparison. It is also interesting to look at the effective number of free electrons in a given energy range as computed from the sum rule $n_{eff}(E)$:

$$n_{eff}(E) = (2m\epsilon_0/\pi e^2\hbar^2)\int_0^E E'\kappa_2(E')\,dE' \,. \qquad (16)$$

It can be seen from Fig.12 that $n_{eff}(E)$ increases almost linearly up to the highest experimental energy with no leveling off at 24 (or 20) electrons/unit cell as might be expected. This is a consequence of further d or p transitions commencing at 9 eV in MnSe and 10 eV in MnS. It is not possible to distinguish between d- and p-electron excitation from a plasma oscillation analysis in the manganese chalcogenides.

The highly damped plasma resonance indicated at 11.5 eV in MnSe must be considered with some caution. Small reflectance errors over broad energy regions can seriously affect the computed optical constants and hence the optical energy-loss function. This consideration is especially important in the present study where reflectometer *in situ* sample preparation was not accomplished. MnS appears not to display a similar structure, although Huffman and Wild's data extend only to 14 eV, so perhaps the resonance is yet to come. The resonance was a persistent effect which appeared in all of the calculated results of the better MnSe samples and so it is assumed to be a real phenomena. However, it would be desirable to perform a fast electron loss experiment to verify the optical electron losses reported here. From the screened plasma frequency relation, Eq. 14, one computes for the 11.5-eV loss peak an effective electron concentration of 38.5 electrons/unit cell. This nearly corresponds to the full p–d electron concentration of 44 electrons/unit cell. Hence, we tentatively ascribe the resonance to a screened joint resonance of the $4p$ selenium valence electrons and the $3d$ manganese electrons. One concludes that by 11.5 eV both the d and p electrons have been excited. If one assumes that the absorption from 2–8 eV is a $p \rightarrow d$ "localized exciton," then presumably the absorption centered at 10 eV is a consequence of electron excitation into the $4s$ state, perhaps $4p \rightarrow 4s$. The $4p$–$4s$ gap is then ~10 eV, which is about 50% larger than band calculations indicate.[38] The excitation of the screening electrons is manifested in the strong absorption at 15 eV. One could reasonably expect to see transitions from the deep-lying selenium $4s$ and $3d$ levels in this region.

In NiO and CoO there are, respectively, 32 and 28 d electrons/unit cell. The d-electron concentration is significantly larger than the p-electron concentration in NiO. Calculation of the optical energy loss function from a new phase-shift dispersion analysis of reported reflectance data[41] yields NiO loss peaks at 7.8, 15.2, and, perhaps, ~26 eV. The position of the last peak is uncertain since it is very near to their high-energy data limit. The computed loss peaks in CoO are at 8.7 and 21.2 eV. The resonances at 7.8 and 8.7 eV in NiO and CoO, respectively, are both highly damped and highly screened. For these peaks, following the screening analysis used for MnS and MnSe, one computes 10.5 and 13.5 electrons/unit cell for NiO and CoO. These values are significantly smaller than the electron concentrations computed for the lowest-energy resonances in MnS and MnSe. These small values could be a consequence of excitation of electrons from a hybrid valence band.[59] However, the damping and screening of these resonances is so strong that the crude analysis used certainly cannot be relied upon to give quantitative results. The higher-energy loss peaks in NiO and CoO are screened relatively weakly; therefore, the simple analysis here should be valid.

The loss peak at 21.2 eV in CoO is apparently analogous to the MnSe loss at 11.5 eV, and corresponds to the joint excitation of the $2p$ and $3d$ electrons. One computes an electron concentration for this screened resonance of 51.1 electrons/unit cell which compares accurately with the known p-d concentration of 52 electrons/unit cell. Apparently, the tentatively identified resonance at ~26 eV in NiO is also to be identified with a joint p-d excitation. For this resonance one computes

an electron concentration of 51 electrons/unit cell which compares reasonably well with the p–d concentration in NiO of 56 electrons/unit cell. The intermediate NiO resonance at 15.2 eV yields, upon analysis, an electron concentration of 26.8 electrons/unit cell. This concentration is only slightly larger than the valence-band p-electron concentration, but it is not at all clear that the resonance can be associated with excitation of the $2p$ valence band electrons in view of the resonance of unknown origin at lower energy.

The MnSe data and the analyses reported here further emphasize the strong general similarity in the optical properties of the antiferromagnetic insulators MnO, MnS, NiO, and CoO. It is likely that a single model can be applied to all of these compounds to describe their electronic structure. Many-body effects are undoubtedly important from the absorption edge to probably the first reflectance minimum. The nature of the excitations present in this range is still not clear. In NiO and CoO it appears that electrons from states not directly corresponding to free ion states may be involved. A more sophisticated analysis and interpretation of the volume plasma resonances in these materials may contribute additional information concerning p and d electron excitation in various energy regions.

ACKNOWLEDGMENTS

The authors would like to thank R. Craig for helpful suggestions in interpreting the results. We have also profited greatly by discussions with H. White, R. Potter, E. Middlemiss, and H. E. Bennett. We also wish to thank Ildiko Kerek, Nancy Rettig, and Judith Decker for assistance in the preparation of this manuscript.

---

†Work supported by the U. S. Air Force Office of Scientific Research.

*Based on a thesis submitted by D. L. Decker in partial fulfillment of the requirements for the Ph.D. degree in Physics at California, Riverside, Calif., 1969.

‡Present address: Michelson Laboratory, China Lake, California 93555.

[1]G. W. Pratt and R. Coelho, Phys. Rev. 116, 2, 281 (1959).

[2]D. R. Huffman, R. L. Wild, and M. Shinmei, J. Chem. Phys. 50, 9, 4092 (1969).

[3]D. R. Huffman and R. L. Wild, Phys. Rev. 156, 989 (1967).

[4]R. R. Heikes, A. A. Maradudin, and R. C. Miller, Ann. Phys. (N. Y.) 8, 733 (1963).

[5]J. Palmer, J. Appl. Phys. 25, 125 (1954).

[6]A. Baroni, Z. Krist. 99, 336 (1938).

[7]H. Z. Shäfer, Z. Anorg. Allgem. Chem. 286, 27 (1956); 286, 42 (1956); 290, 279 (1957); 291, 221 (1957); 291, 254 (1957).

[8]R. Nitsche, H. U. Bolsterli, and M. Lichtensteiger, J. Phys. Chem. Solids 21, 199 (1961); see also, R. J. Nitsche, *ibid.* 17, 163 (1960).

[9]Johnson, Matthey, and Co., London.

[10]American Smelting and Refining Co., South Plainfield, New Jersey.

[11]H. Wiedemeier and W. Goyette, J. Chem. Phys. 48, 7, 2936 (1968).

[12]Commercial analysis by Gulf General Atomic, San Diego, California.

[13]J. L. Richards, *The Use of Thin Films in Physical Investigations*, edited by J. C. Anderson (Academic, New York, 1966).

[14]G. Saum and E. Hensley, Phys. Rev. 113, 1019 (1959).

[15]M. Hass, Phys. Rev. 117, 1497 (1960).

[16]M. Born and K. Huang, *Dynamical Theory of Crystal Lattices* (Oxford U.P., Oxford, England, 1954).

[17]H. J. Bowlden and J. K. Wilmshurst, J. Opt. Soc. Am. 53, 9, 1073 (1963).

[18]F. Stern, *Solid State Physics* (Academic, New York, 1963), Vol. 15.

[19]M. Gottlieb, J. Opt. Soc. Am. 50, 343 (1960).

[20]G. Andermann, A. Caron, and D. A. Dows, J. Opt. Soc. Am. 55, 1310 (1965).

[21]D. W. Berreman, Phys. Rev. 163, 855 (1967).

[22]Electronic Space Products, Inc., Los Angeles, California.

[23]R. Lyddane, R. Sachs, and E. Teller, Phys. Rev. 59, 673 (1941).

[24]B. Szigeti, Trans. Faraday Soc. 45, 155 (1949); Proc. Roy. Soc. (London) A204, 51 (1950).

[25]J. R. Tessman, A. H. Kahn, and W. Shockley, Phys. Rev. 92, 890 (1953); see also, A. Ruffa, *ibid.* 130, 1412 (1963).

[26]The polarizability of Mn^{2+} should be quite close to that of Fe^{2+}, which Tessman, Kahn, and Shockley give as -1.0×10^{-24} cm^3.

[27]B. Dick and A. Overhauser, Phys. Rev. 112, 90 (1958).

[28]J. C. Phillips, Phys. Rev. 166, 3 (1968); 166, 832 (1968); 168, 3 (1968); 168, 905 (1968); 168, 912 (1968); 168, 917 (1968).

[29]R. Neuman, and R. M. Chrenko, Phys. Rev. 114, 1507 (1959).

[30]Y. Mizuno and S. Koide, Physik Kondensierten Materie 2, 166 (1964).

[31]S. Sugano and Y. Tanabe, *Magnetism*, edited by T. Rado and H. Suhl (Academic, New York, 1963), Vol. III.

[32]K. K. Kelley, J. Am. Chem. Soc. 61, 203 (1939).

[33]Preliminary specific-heat measurements accomplished in conjunction with the present study yielded a Néel temperature of 247 °K.

[34]J. F. Dillon, Jr., *Magnetism*, edited by T. Rado and H. Suhl (Academic, New York, 1963), Vol. III.

[35]Y. Tanabe and S. Sugano, J. Phys. Soc. Japan 9, 766 (1954).

[36]L. E. Orgel, J. Chem. Phys. 23, 1004 (1955).

[37]D. Reinen, Ber. Bunsenges Physik. Chem. 69, 82 (1965).

[38]T. M. Wilson, J. Appl. Phys. 40, 1588 (1969).

[39]S. Van Houten, J. Phys. Chem. Solids 17, 7 (1960).

[40]R. J. Powell, Ph.D. thesis (Stanford University, 1967) (unpublished).

[41]R. J. Powell and W. E. Spicer, Phys. Rev. B 2,

2182 (1970).
[42]S. Wemple and M. DiDomenico, Jr., Phys. Rev. Letters 23, 1156 (1969).
[43]H. R. Philipp and H. Ehrenreich, Phys. Rev. 129, 1550 (1963); 131, 2016 (1963); 131, 2016 (1963).
[44]M. Cardona and D. L. Greenaway, Phys. Rev. 133, A1685 (1964).
[45]T. M. Donovan, E. J. Ashley, and H. E. Bennett, J. Opt. Soc. Ann. 53, 12 (1963); 53, 1403 (1963).
[46]H. E. Bennett and J. O. Porteus, J. Opt. Soc. Am. 51, 123 (1961).
[47]D. R. Huffman (private communication).
[48]D. M. Roessler, Brit. J. Appl. Phys. 16, 1119 (1965).
[49]I. Drabkin, L. Emel'yanova, R. Iskenderov, and Ya. Ksendzov, Fiz. Tverd. Tela 10, 3082 (1968) [Sov. Phys. Solid State 10, 2428 (1969)].
[50]Photoconductivity measurements performed by E. R. Middlemiss, University of California, Riverside, Calif.
[51]W. E. Spicer, Phys. Rev. 154, 385 (1967).
[52]D. Adler, IBM J. Res. Develop. 14, 261 (1970).
[53]L. Marton, Rev. Mod. Phys. 28, 172 (1956).
[54]D. Pines, *Elementary Excitations in Solids* (Benjamin, New York, 1963).
[55]S. L. Adler, Phys. Rev. 126, 413 (1962).
[56]H. Ehrenreich and H. R. Philipp, *Proceedings of the International Conference on the Physics of Semiconductors, Exeter* (The Institute of Physics and Physical Society, London, 1962).
[57]C. B. Wilson, Proc. Phys. Soc. (London) 76, 481 (1960).
[58]H. Ehrenreich and H. R. Philipp, Phys. Rev. 128, 1622 (1962).
[59]J. L. McNatt, Phys. Rev. Letters 23, 915 (1969).

PHYSICAL REVIEW B VOLUME 4, NUMBER 10 15 NOVEMBER 1971

Third-Harmonic Generation in Absorbing Media of Cubic or Isotropic Symmetry*

W. K. Burns† and N. Bloembergen
Division of Engineering and Applied Physics, Harvard University, Cambridge, Massachusetts 02138
(Received 14 May 1971)

Third-harmonic generation in strongly absorbing media has been measured in reflection, by means of a picosecond pulse train from a mode-locked Nd-glass laser. The nonlinear susceptibility $\chi^{(3)}(3\omega)$ has been measured in the semiconductors diamond, Si, Ge, and GaAs, and the metals Be, Mg, Al, Cu, Ag, and Au relative to LiF. The data are compared with data for $\chi^{(3)}$ obtained in the infrared from frequency mixing with CO_2 lasers. The different dispersion characteristics for valence- and conduction-band contributions are pointed out. The cubic anisotropy of $\chi^{(3)}(3\omega)$ in silicon and several alkali halide crystals is determined by means of circularly polarized laser pulses. The selection rules for the generation of circularly polarized third harmonics have been confirmed both in transparent and in absorbing media.

I. INTRODUCTION

Optical third-harmonic generation (THG) in transmission was first detected by phase matching in calcite by Terhune *et al.*[1] They also measured the susceptibility and anisotropy in LiF and other alkali halide crystals.[2] THG in gases was observed by New and Ward.[3] They discovered that phase-cancellation effects from focusing into a homogeneous medium of infinite extent eliminate THG. Phase-matched THG was achieved in a liquid by Bey *et al.*[4] by utilizing the anomalous dispersion due to dye molecules placed in a normally dispersive liquid. The same workers also observed THG in reflection from the same dye-liquid combination by achieving phase matching near the critical angle for total internal reflection.[5] Non-phase-matched THG in reflection was observed by Wang and Baardsen,[6] who remeasured TH susceptibilities for the alkali halides and glass. The first reflected THG from strongly absorbing media was reported by Bloembergen *et al.*[7]

The observed signals are necessarily weak, since they are generated by a higher-order nonlinear polarization in the small absorption depth at the third-harmonic frequency. The intensity of the incident laser light must be high, and yet thermal damage due to absorption cannot be tolerated. If the medium is also strongly absorbing at the fundamental, the use of high-intensity picosecond laser pulses is essential. In this paper more details on the experimental method and more complete experimental data are presented. The dispersion of the nonlinear susceptibility in the absorbing frequency ranges is of theoretical interest.

In Sec. II the pertinent theory of THG in reflection and transmission is briefly reviewed. Section III describes the experimental techniques. In Sec. IV we present the experimental results for some semiconductor crystals of cubic symmetry, including diamond, Si, Ge, and GaAs. The dispersive behavior of $\chi^{(3)}$ is discussed and a comparison with other data for $\chi^{(3)}$ obtained from frequency mixing in the infrared is made. The influence of conduction electrons and surface preparation is investigated. In Sec. V the cubic anisotropy of $\chi^{(3)}$ in